Peter Oppermann and Christian Renner. Low-Power Ultrasonic Wake-Up and Communication through Structural Elements. In Proceedings of the 7th International Workshop on Energy Harvesting & Energy-Neutral Sensing Systems (ENSsys'19), November 10, 2019, New York, NY, USA.

Low-Power Ultrasonic Wake-Up and Communication through Structural Elements

Peter Oppermann
peter.oppermann@tuhh.de
Hamburg University of Technology
Hamburg, Germany

Christian Renner
christian.renner@tuhh.de
Hamburg University of Technology
Hamburg, Germany

ABSTRACT

Research in ultra-low energy communication for wireless sensor networks mostly focuses on radio frequency (RF). Simple, low-cost, and low-power approaches for acoustic communication are typically not explored, although in a variety of applications acoustic communication using ultrasonic waves is preferable to RF. In others, motes are already equipped with sensors and actuators for acoustics. In this work, we present a method to communicate between motes on structural elements using piezoelectric discs. We demonstrate that data rates up to one kilobit per second are achievable with only minimal additional hardware. At the same time, the energy consumption for communication is reduced compared with popular RF methods.

CCS CONCEPTS

• **Hardware** → *Sensor devices and platforms*; *Wireless devices*; **Signal processing systems**.

ACM Reference Format:
Peter Oppermann and Christian Renner. 2019. Low-Power Ultrasonic Wake-Up and Communication through Structural Elements. In *7th International Workshop on Energy Harvesting & Energy-Neutral Sensing Systems (ENSsys'19), November 10, 2019, New York, NY, USA.* ACM, New York, NY, USA, 7 pages. https://doi.org/10.1145/3362053.3363490

1 INTRODUCTION

Typical applications for wireless sensor networks (WSN) have to work on a minimal energy budget, e.g., because they are supplied by energy-harvesting or because battery size and weight are restricted. Communication is often one of the most energy-demanding tasks in such applications, and hence, energy-conserving communication techniques are crucial for WSNs.

Radio-Frequency (RF) based communication is the de-facto standard for WSNs, and various techniques have been investigated to reduce its energy demand, e.g., backscattering [8, 14] and wake-up radios [4] (WuR). However, in some cases, RF is not favorable or even impossible. Such applications include sensors placed inside a metallic housing or in underwater or underground [1, 12] environments. Communication through compartments of naval vessels [11] and sensors within pressurized containers [2] are well-known scenarios.

Another field of interest, however, is structural health monitoring, where motes need to exchange data to synchronize measurements or to transmit results. On structures like bridges, the devices may be shielded, e.g., by metallic beams. For nondestructive testing techniques such as vibro-acoustic modulation [3], these motes are equipped with sensors and actuators for ultrasonic waves already. If ultrasonic communication replaces RF, the cost and size of motes decrease by reusing the existing components. Further, metals exhibit excellent conductance of acoustic waves and form a waveguide. Therefore, it might even be more energy efficient to exploit resonance effects in metallic structures with acoustic communication instead of RF.

While the possibility to transmit data across thin steel plates was already demonstrated [2, 11], we investigate acoustic communication techniques for longer distances, e.g., along metallic beams, particularly for ultra-low energy applications. Therefore, we transfer the concept of WuR from RF to ultrasonic communication. A WuR almost eliminates the receiver's need for idle listening without introducing additional delays as in duty-cycling. The total energy demand for communication can thereby be reduced by several orders of magnitude [4] while still providing sufficient quality of service. More specifically, our contributions are:

- Development of an acoustic WuR that consumes only a negligible amount of energy during idle listening.
- Presentation of a simple communication method based on WuRs, that uses bursts of ultrasonic waves in metals and supports selective wake-up and data transmission.
- Analysis of the capabilities of this method on different specimen and analysis of the influencing factors on the achievable data rate and reliability of communication.
- Theoretical analysis of the energy demand for acoustic communication and comparison to standard RF-based methods.

2 RELATED WORK

To the best of our knowledge, no prior work exists, that matches our approach. The ultrasonic communication techniques described in the literature differ in one or more of the following criteria: They employ *a)* a high bit rate communication, which is not suitable to low-power motes, or *b)* an asymmetric architecture, where either sender or receiver is a high-power device, or *c)* ultrasonic communication through a different type of channel, or *d)* don't support wake-up.

The acoustic communication methods investigated in [2, 11] and [5] focus on communication across a metal wall, where a much simpler and shorter channel is encountered.

ENSsys'19, November 10, 2019, New York, NY, USA

ACM ISBN 978-1-4503-7010-3/19/11…$15.00
https://doi.org/10.1145/3362053.3363490

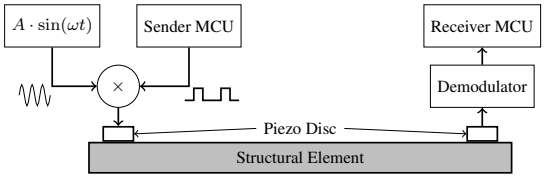

Figure 1: Principle setup for acoustic communication over a physical structure.

Alternatively, [9] does focus on acoustic data transmission over longer distances through pipelines. However, both [9], and [5] only employ methods with a high power sender, which establish either only one-way communication or the low-power device uses a backscattering approach. In [1], the authors used a similar acoustic communication scheme, but also established only one-way communication with a low-power sender.

None of the mentioned sources focuses on applications, where both sender and receiver operate on ultra-low energy with a quasi-passive demodulator, and none explores the influences of structural elements on the signal.

3 WAKE-UP PRINCIPLE

The demonstrated communication system is shown in Fig. 1. It consists of a sender that introduces short bursts of an acoustic sinusoidal wave into the structure using a piezoceramic disc. An identical piezo disc at the receiver produces a charge upon deformation, which we can measure as a voltage.

The voltage, however, is not observed actively, e.g., sampled regularly by a microcontroller unit (MCU), since that would continuously need power. In contrast, we employ a virtually passive ($P < 400\,\text{nW}$) circuit to detect the presence of a burst and provide a digital signal from decoding presence and absence of bursts. A microcontroller can then consume the digital signal using GPIO interrupts to wake up from sleep mode.

Subsequently to the wake-up bursts, the same mechanism can be employed to transmit several bursts, which encode a digital message. Here, the binary symbols, one and zero, are modulated by the presence or absence of a burst in a symbol period of length T_s. This simple form of modulation resembles on/off-keying (OOK), which is a form of amplitude modulation.

More sophisticated modulation schemes exhibit certain advantages over OOK. Frequency modulation techniques, for example, are less susceptible to noise but need more complex hardware for demodulation. The requirement for simple, low-cost, and low-power hardware motivates the choice of OOK in this general feasibility study.

In the remainder of this section, we first investigate the generation of bursts and which parameters affect the acoustic waves in the structure. Then we show a hardware implementation of a demodulator, that can detect the bursts and convert them back into digital symbols for the receiver MCU to read.

3.1 Burst Generation

When using acoustic waves in metals, resonance effects are far more influential than in classical RF communication. The main reason for that is that the metallic structure acts as a waveguide. The waves are nearly entirely reflected at the interfaces between metal and the surrounding air due to the vast difference in acoustic impedance. Therefore, the choice of the frequency of the sinusoidal burst is strongly affecting the signal strength at the receiver.

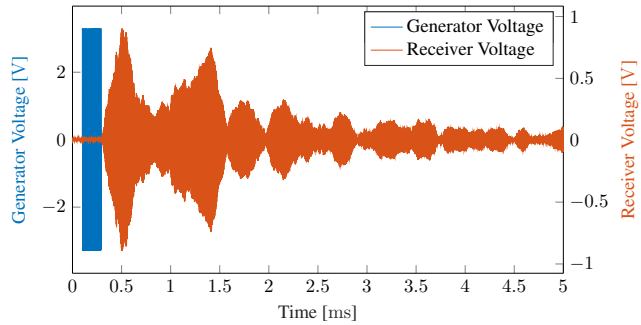

Figure 2: Excitation voltage at the sender piezo and open-circuit voltage on the receiver piezo after a 300 µs burst in a resonant frequency.

Reverberation can be beneficial since it allows us to use a small excitation at the sender piezo and still generate a strong signal at the receiver due to the positive interference of reflections. The sending power required to generate a detectable signal at the receiver can thereby be reduced.

Figure 2 shows the voltage at the receiver piezo when a 300 µs burst with a frequency of 207 kHz is introduced into a specimen. We describe the detailed experiment setup in Section 4. Note that the voltage amplitude at the receiver is delayed significantly due to the speed of sound in the specimen, and then builds up over time until it reaches its maximum at 0.9 V. This build-up is an effect of positive interference.

The carrier frequency for the bursts resulting in the highest output voltage at the receiver piezo for a given input excitation depends on many factors: The piezo discs work most efficiently in a specific frequency range, but also the geometry and material of the structure play an important role. Finally, the placement of the piezo discs, i.e., the distance between the piezo discs and how they are attached to the surface, can also influence the resonant frequency. Therefore, we chose to empirically identify the resonant frequency for the combines system of the sender, specimen, and receiver by systematically sweeping over a range of frequencies and choosing the one yielding the highest peak amplitude at the receiver piezo.

3.2 Demodulator

The demodulator depicted in Fig. 3 has been developed to detect the sinusoidal bursts in the structure at the receiver. The voltage over the piezo disc is rectified using a bridge rectifier. On the occurrence of a burst, capacitor C_1 is charged. The capacitor C_{pd} and the Diode D_{pd} form a peak detector so that V_{th} follows V_1 and poses a dynamic threshold. R_1 has been introduced to ensure quick discharge of C_1 when a burst is over so that the demodulator can detect the next burst, while R_{pd} should slowly discharge C_{pd} to lower the threshold when no bursts occur over time.

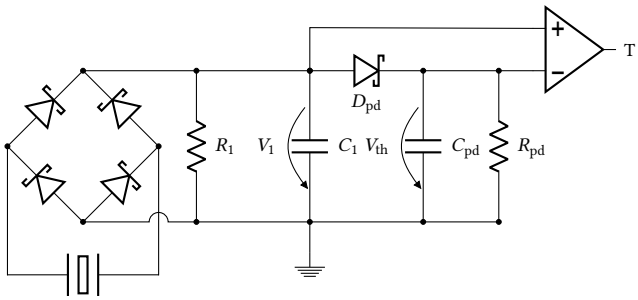

Figure 3: The demodulator circuit resembles a simple energy harvester and a peak detector. Comparing the harvester's voltage and the peak detector's voltage, a short vibrational burst on the line can be detected.

If V_1 is considerably higher than the threshold V_{th}, it is likely that a burst has occurred, while the other way round implies, that the voltage produced by the piezo is decreasing, hence a burst has just ended. In an idle state, V_1 and V_{th} are close to equal. We use the STMicroelectronics TS882 comparator to generate a binary signal, our bitline, from these voltage differences. This comparator is the only active device in this circuit and hence has to be powered externally. However, its typical current consumption is only about 220 nA [13] and is therefore negligible compared to typical MCUs in sleep mode.

The parameters of this circuit need to be adjusted carefully to achieve an appropriate balance of sensibility, specificity, and transmission speed. Sensibility, in this case, means that the demodulator can already detect short and low-energy pulses, which reduces the necessary sender power. Specificity, on the other hand, means that the demodulator should not be triggered easily by noise. These two properties mainly depend on the capacitance of C_1. The demodulator has to return to a logic 0 quickly and reliably after detecting a burst so that it can distinguish the next pulse from the previous one at high data rates.

To find a good set of parameters, we performed a mix of simulation and experimental testing. We sent a series of short bursts through a steel beam, each 400 µs long, and observed V_1, V_{th} and the comparator output with an oscilloscope. The results for our chosen set of parameters are shown in Fig. 4. Note that every spike of V_1 produces a distinguishable pulse that the comparator can detect. However, the pulses are not regular: When the charge on C_{pd} is low at the start of a burst, the time until V_1 drops below V_{th} is considerably longer than with a high V_{th} at the start of a burst. The maximum pulse duration directly yields the minimum time between two adjacent pulses, so that they are distinguishable for the receiver. In this case, it must be at least 1 ms.

3.3 Challenges

In a real-world application, depending on the target structure, there might be many sources of noise introducing unintended bursts of energy into the structure. Therefore it is highly desirable to not only send a single burst as a wake-up signal but a predefined preamble, which reduces the amount of false-positive wake-ups. Selective

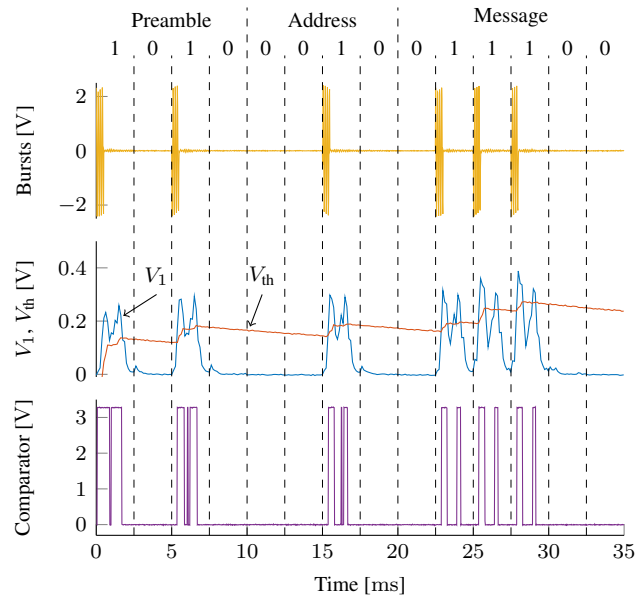

Figure 4: Voltage at the sender piezo (top), voltages V_1 and V_{th} at the demodulator (middle) and resulting comparator output (bottom). Dashed lines delimit the symbol periods. The chosen parameters are C_1 = 10 nF, C_{pd} = 100 nF and R_1 = 10 kΩ. R_{pd} has been omitted.

wake-up can also be achieved by assigning identifiers to the nodes and sending the addressee's identifier following the preamble. Then, the receiver can reduce overhearing to only a few bits.

Unfortunately, Fig. 2 shows that reverberation is considerable. While the first peak's amplitude is about 700 mV, the first echo peak still reaches about 600 mV. The echoes persist within the specimen for several milliseconds after the burst has stopped, which leads to inter-symbol interference if the symbol period is not chosen long enough and therefore reduces the achievable data rate.

Reverberation can also be seen when inspecting V_1 in Fig. 4: directly after a burst, it is not just spiking once and then dropping smoothly. These echo spikes sometimes can—depending on the exact situation (pulse strength, charge level on C_1 and C_{pd})—push V_1 over V_{th} multiple times during one symbol time. Therefore, to obtain reliable communication, the time between subsequent sender pulses should be chosen long enough to avoid inter-symbol interference by echoes.

A typical technique to mitigate reverberation with OOK is frequency hopping, which would require multiple burst frequencies and the possibility to filter at the receiver. Because of the strong dependence of frequency on the received signal strength in this case, and because of the focus on simplicity, we did not consider frequency hopping here.

3.4 Communication Protocol

In Section 3, we have described how a short burst of an acoustic wave can be detected with low-power hardware so that a microcontroller can be woken up. Now, we will design a protocol, in

Table 1: Dimensions and Material of the specimen and distance between centers of the piezo discs of sender and receiver motes.

Spec.	Material	Length	Width	Height	Distance
1	Steel	1000 mm	20 mm	10 mm	885 mm
2	Aluminum	480 mm	71 mm	5 mm	374 mm
3	Aluminum	300 mm	20 mm	4 mm	61 mm

which several of these pulses are chained to transmit a message from one sensor node to another. Our primary requirement is a simple, low-power decoding mechanism. To achieve this simplicity in sender and receiver implementation, we have decided to employ OOK. Each symbol is a single bit, where a burst during the symbol time encodes a logic one, and the absence of a pulse encodes a logic zero.

The full transmission consists of a preamble, an address, and a payload (see Fig. 4). The receiver can use the preamble to distinguish a valid message from a pulse produced by other sources such as noise. After the preamble, a four-bit node address is sent to identify the receiver of the wake-up, followed by the payload.

Unlike in classical OOK, the duration of the pulses that are generated by the comparator varies. The initial pulses are rather long, but once C_{pd} is charged, the pulse duration shrinks. Additionally, multiple short pulses may appear during one symbol time due to echoes. Here, the timing of the rising edges can be controlled much more precisely by the sender than the timing of the falling edges. Therefore, a decoder implementation must synchronize the start of the symbol periods using the rising edges in the preamble.

4 EXPERIMENTAL EVALUATION

In this section, we show a setup to evaluate the presented communication method. We have conducted test runs showing bit error rates (BER) for different specimens and different parameters of the sender and receiver. We examined three specimens on which the piezo discs were attached to the surface using an epoxy adhesive. They differ in dimension, geometry, and material. The details are shown in Table 1. For both materials, we have measured the speed of sound. In aluminum, the signal travels with $c = 4794\,\mathrm{m\,s^{-1}}$, and in the steel specimen, it travels with $c = 4538\,\mathrm{m\,s^{-1}}$.

Variable parameters are the symbol duration T_s, the amplitude of the sinusoidal burst generated by the sender V_{b}, which is given as peak voltage, the duration of bursts T_{b} and the frequency of the burst f_{b}.

A decoder on an STM32F446 development board has been implemented, with an ARM Cortex M4. The decoder is in sleep mode until a GPIO interrupt from the bitline of the demodulator triggers a wake-up. At this moment, a timer is configured to trigger a regular interrupt after every T_s. At the same time, rising and falling edges are counted also using interrupts. After each T_s, the decoder performs a bit decision: The bit is a zero if no rising edges have been counted during this T_s, or a one if one or more rising edges have been counted. Only when the first four bits—the preamble—have been detected successfully, the decoder reads a message of a fixed,

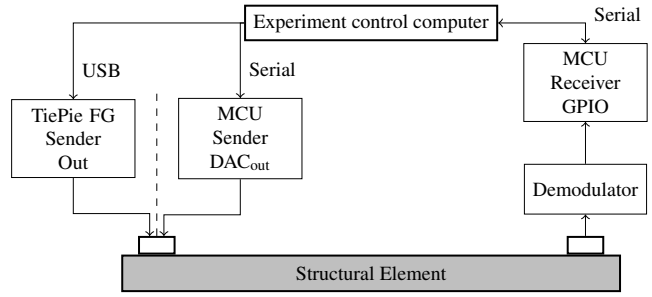

Figure 5: Evaluation setup showing the components used. As sender, either a microcontroller can be used to generate the input voltage for the piezo or a USB controllable function generator.

pre-configured length. In our tests, we have arbitrarily chosen a packet length of 25 Byte, or 200 Bit, respectively.

We made two implementations of the sender. One implementation is also using an STM32F446 microcontroller as sender MCU. It precomputes the samples for a sine wave for the onboard digital to analog converter (DAC) with a given V_{b} and T_{b} and stores them in a buffer. The MCU can remain in sleep mode most of the time and only wakes up every T_s. Then, if the current bit is a one, it uses the DAC to produce a burst and then goes back to sleep mode. Unfortunately, the DAC can not use its full voltage range with such high frequencies. Therefore, V_b is limited to lower amplitudes.

For evaluation purposes, we implemented an alternative sender using a USB function generator. The function generator has the advantage that it is more flexible and can produce a broader range of voltages and frequencies than the MCU-based sender.

4.1 Communication Method

For assessment of the reliability and robustness of the proposed communication method, packets of fixed length with randomly generated content were sent through the metal specimen to the receiver with different sets of parameters. Later, we calculated the BER from the received messages. In case the receiver can not detect the preamble and hence does not record a message, all bits of the message are considered wrong. These missed packages lead in some cases to a BER higher than 0.5.

Expectations for the parameters are that an increase in V_{b} or an increase in burst duration T_{b} reduces BER since more energy is used to transmit the signal. Further, we would expect an increase in symbol duration T_{s} also to lower the BER because of reduced inter-symbol interference. The following evaluation has been made using the USB function generator as sender. However, we have also verified the same experiment with the MCU implementation of the sender within the feasible voltage range (< 1 V amplitude). These results were consistent with the results from the function generator implementation.

4.1.1 Influence of Sender Parameters. Figure 6 shows an evaluation of the BER in specimens 1, 2, and 3 at different V_{b}, T_{b}, and T_{s}. Here, it can be seen, that a low burst voltage and a short burst duration (bottom left corner of each heatmap) lead, independent

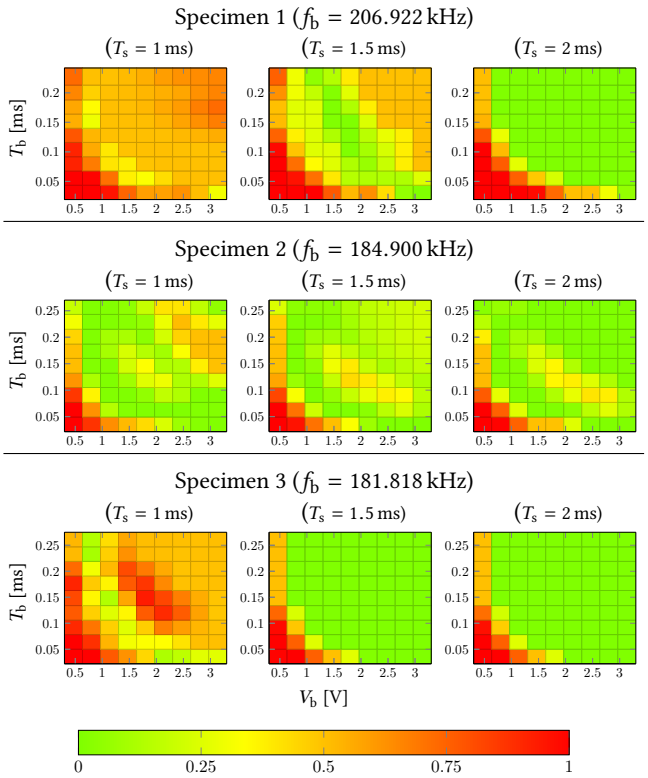

Figure 6: Bit error rates (BER) for the different specimens at resonance frequency with different burst lengths T_b and burst voltages V_b. Parameters have to be chosen carefully to achieve a low BER at high data rates.

of the symbol time, to a BER close to one. This observation is not surprising since the bursts are so weak that the receiver can not even detect the preamble.

However, with a low $V_b = 0.5$ V, BERs of zero can be achieved, if only the burst duration is increased. At the same time, with a short burst duration, a low BER can be achieved by increasing V_b. Note that further increasing V_b or T_b does not necessarily lead to a lower BER. Especially in case of a short symbol time (left column), it instead leads to a higher BER. Much likely, this is an effect of increased inter-symbol interference: The echoes also scale with the increasing energy of the original bursts. Hence, this effect diminishes with longer T_s, because then there is enough time after a burst for the echoes to fade out before the next symbol is sent.

These results show that when choosing a low data rate, ultrasonic communication is reasonably robust: Most combinations of burst voltages and durations work well and produce BERs close to or equal to zero. However, if a higher data rate is desired, T_s must be small, V_b and T_b need to be chosen carefully to achieve reliable communication.

4.1.2 Influence of Specimen Dimensions. Figure 6 (top) shows the BERs for specimen 1. Compared to the other two specimens, BERs close to zero can not be achieved for $T_s = 1$ ms. Also for $T_s = 1.5$ ms, only very few parameter sets perform well. For specimen 1, the biggest one, we can also observe that a higher burst voltage or longer burst durations are needed for the receiver to detect the preamble at all.

At this time, we can not say with certainty, how specimen dimensions and data rates are related. The number of specimens under test vary in all three dimensions and even in the material. Since steel and aluminum exhibit different damping properties on acoustic waves, the material also influences reverberation. As a next step, a theoretical analysis of the types of the excited waves and their behavior in the specimen will allow more insight.

4.2 Energy Considerations

In this section, we present an estimation of the energy demand for acoustic communication and compare it to the energy demand of established techniques of RF communication. Since this work's main goal is to explore the general feasibility and limitations of acoustic communication in the context of WSNs, our choice for the MCU, the STM32F446 was motivated by its ease of use and flexibility.

However, using the knowledge gained, we perform a theoretic estimation about the energy consumption with an ultra-low energy MCU that is sufficient to perform the sending and receiving tasks. A good option for an MCU is the PIC12LF1552 [7] also used in [4] for a similar task. This 8-bit MCU, clocked with 8 MHz, consumes $P_{\mathrm{MCU,s}} = 36$ nW in sleep mode and $P_{\mathrm{MCU,a}} = 432\,\mu$W.

For the estimation, we assume that a message with 64 bytes payload is sent from sender to receiver node. As sender parameters, we assume $T_s = 1$ ms, $f_b = 200$ kHz, $T_b = 100\,\mu$s, and $V_b = 1$ V. With these parameters, the reception of a package including preamble takes $T_{\mathrm{pkg}} = 516$ ms.

4.2.1 Burst Generation and Sending. During the generation of a burst, the power used to drive the piezo disc has to be considered. For the specimen and piezo discs in use, we have measured the current draw during a burst at $V_b = 1$ V and $f_b = 200$ kHz by measuring the voltage drop over a 10 Ω resistor in series with the piezo. The result is an effective current of $\hat{i}_{\mathrm{p,b}} = 605\,\mu$A resulting in a power of $P_{\mathrm{p,b}} = 428\,\mu$W.

Due to the mainly capacitive nature of piezos, $P_{\mathrm{p,b}}$ increases quadratically with V_b. We observe in Section 4.1.1 that a stronger signal at the receiver can not only be generated by increasing the voltage at the sender, but also by increasing the burst duration. Since a prolonged burst does not change the power and increases the burst energy linear, it is preferable to increase burst duration rather than sending voltage to achieve a low energy demand.

The sender needs to be able to generate a sinusoidal burst, which requires, that the sender MCU has a DAC or an external function generator. In our implementation, we noticed that frequencies in the range of 200 kHz, which have shown to work best, can only be generated with a powerful MCU, that can generate several megasamples per second on its DAC. Such an MCU, however, needs much energy. A better option could be, to use a dedicated function generator IC, such as the Analog Devices AD9837, in combination with a low-power MCU.

According to its datasheet [6], the function generator uses about $P_{\mathrm{FG}} = 8.5$ mW when active. In total, the energy demand for sending a standard package is then given by the energy demand in sleep

mode plus the energy used for burst generation. We assume the average packet to have equally distributed ones and zeros as bits. Therefore the number of bursts N_b is half the number of bits per packet. This results in a sending energy per packet of

$$E_{\text{send}} = T_{\text{pkg}} P_{\text{MCU,s}} + N_b T_b \cdot (P_{\text{FG}} + P_{\text{p,b}}) = 230\,\mu\text{J}. \quad (1)$$

4.2.2 Receiver Requirements. The decoding of the received signal is relatively simple. No active sampling and no complex computations are involved. The receiver MCU can stay in a low-energy sleep mode while no message is transmitted and wait for a GPIO interrupt on the bitline. During the reception, it needs to count rising edges on the bitline and perform a bit decision based on the presence of rising edges every T_s. Both tasks can also be achieved using GPIO and timer interrupts, while the MCU remains in sleep mode most of the time.

In addition to the MCU power consumption, the comparator used in the demodulator, an STMicroelectronics TS882, typically needs $P_c = 396\,\text{nW}$ [13].

When using the proposed ultra-low power MCU, even if we assume that the MCU is active during the whole reception time, the receiver would need

$$E_{\text{rec}} = T_{\text{pkg}} \cdot (P_{\text{MCU,a}} + P_c) = 222\,\mu\text{J}. \quad (2)$$

5 DISCUSSION

According to the measurements from [10], we calculated the raw energy demand of an off-the-shelf IEEE 802.15.4 transceiver at 0 dB sending power. The reception of an equally sized 64 bytes package would need 450 µJ while the transmission needs 366 µJ. In sum this yields about twice as much energy demand as our estimation of what acoustic communication would need if implemented with low-power MCUs. Although the comparison is not entirely fair—the transceiver also performs higher layer protocol functions, e.g., CSMA—these results show that the energy demand of a prototype for acoustic communication is already in the same order of magnitude as highly optimized RF technology.

While this analysis shows only the energy need for the transmission of a single package, an immense advantage of the presented method is the wake-up functionality. In [4], an RF-based WuR has been implemented, and its energy consumption within a network has been analyzed. Compared to state-of-the-art duty cycling approaches, the energy consumed by the network could be reduced by several orders of magnitude, especially when the interval between messages is long (> 10 s). The same advantage over classical, duty-cycling based communication systems can be achieved using the presented acoustic WuR.

When it comes to data rate and latency, the presented method shows clear disadvantages over state-of-the-art RF standards. Based on the limitations of the speed of sound in metals and the low achievable data rates, the transmission of a 64 bytes package takes roughly 0.5 s, while in IEEE 802.15.4 the same packet can be transmitted in about 3.5 ms. The range can not be compared at this stage since tests on bigger structures yet have to be performed.

The prototype shows, that low-power acoustic communication is possible and therefore enables communication for WSNs in environments unsuitable to RF. Moreover, the results show that acoustic communication is a promising alternative to RF in WSNs with matching requirements on data rates and latencies. Further, it permits reuse of available vibration sensing and generating hardware for communication and hence enables cheaper and smaller motes with only minimal additional hardware needed for demodulation.

6 FUTURE WORK

Based on the positive results from the demonstrated prototype, the acoustic WuR triggers exciting new research opportunities to improve performance in terms of data rate and to research applicability in real-world structures.

Mitigating the effect of reverberation can increase the data rate. Software-based filtering results in much higher hardware and energy requirements and is therefore not considered. A promising option is to perform active noise canceling at the sender, as shown in [11]. This method, however, requires characterization of the specimen's transfer function, which is then employed to calculate the optimal pulse for canceling the echoes.

Fortunately, in the targeted application scenario, the structure and the position of the sensor nodes do not change over time. Hence, optimal sender parameters and cancellation pulse need only be computed once during deployment. In the same way, also the best burst frequency or even multiple resonant burst frequencies can be precomputed. The latter case would even enable frequency hopping.

As demonstrated, the described method, if performed on ultra-low energy MCUs, can be more efficient than standard RF techniques. However, we will implement a real solution using such devices to validate the theoretical advantages in a real-world experiment. Furthermore, we have produced the results presented in this work on rather simple geometries and limited dimensions of specimens. Tests on real-world structures have to be carried out to assess the method's practical applicability. Further, the influence of noise, e.g., induced by traffic on a bridge, is yet unclear.

7 CONCLUSION

The motivation of this work was to explore the possibilities and boundaries of using acoustic communication through structural elements for wake-up and data transmission in WSNs. We have demonstrated, that a standard MCU using the on-chip DAC can generate an acoustic signal strong enough to wake up another node. We have shown that it is generally possible to compensate for a low sending voltage by sending longer bursts and by using resonance effects. We presented a demodulator with ultra-low power usage, that can wake up a microcontroller and demodulate a signal without actively sampling. Transmission of data with up to one kilobit per second through a steel beam over a distance of about one meter was achieved.

Further, we analyzed the influences of different factors, such as dimensions of the beam and sending voltage on the signal transmission and estimated the energy demand of the communication method, where we have shown, that the presented method can be implemented in a more energy-efficient way than standard IEEE 802.15.4 RF communication.

REFERENCES

[1] Christoph Bacher, Peter Palensky, and Stefan Mahlknecht. 2005. Low cost data transmission via metallic solids for sensor networking. In *Proceedings of the IEEE*

Symposium on Emerging Technologies, 2005. 193–198. https://doi.org/10.1109/ICET.2005.1558879

[2] David J. Graham, Jeffrey A. Neasham, and Bayan Sharif. 2011. Investigation of Methods for Data Communication and Power Delivery Through Metals. *IEEE Transactions on Industrial Electronics* 58, 10 (Oct. 2011), 4972–4980. https://doi.org/10.1109/TIE.2010.2103535

[3] Dimitri M. Donskoy and Alexander M. Sutin. 1998. Vibro-Acoustic Modulation Nondestructive Evaluation Technique. *Journal of Intelligent Material Systems and Structures* 9, 9 (Sept. 1998), 765–771. https://doi.org/10.1177/1045389X9800900909

[4] Dora Spenza, Michele Magno, Stefano Basagni, Luca Benini, Mario Paoli, and Chiara Petrioli. 2015. Beyond duty cycling: Wake-up radio with selective awakenings for long-lived wireless sensing systems. In *2015 IEEE Conference on Computer Communications (INFOCOM)*. 522–530. https://doi.org/10.1109/INFOCOM.2015.7218419

[5] Gary J. Saulnier, Henry A. Scarton, Andrew J. Gavens, David Shoudy, M. Wetzel, S. Roa-Prada, T. L. Murphy, and Pankaj Das. 2006. *Through-Wall Communicatin of Low-Rate Digital Data Using Ultrasound*. Technical Report LM-06K102. Knolls Atomic Power Laboratory (KAPL), Niskayuna, NY. https://www.osti.gov/biblio/893018

[6] Analog Devices Inc. [n.d.]. AD9837. https://www.analog.com/media/en/technical-documentation/data-sheets/AD9837.PDF. Accessed: 2019-08-16.

[7] Microchip Technology Inc. [n.d.]. PIC12LF1522. http://ww1.microchip.com/downloads/en/DeviceDoc/40001674F.pdf. Accessed: 2019-08-13.

[8] Jue Wang, Haitham Hassanieh, Dina Katabi, and Piotr Indyk. 2012. Efficient and Reliable Low-power Backscatter Networks. In *Proceedings of the ACM SIGCOMM 2012 Conference on Applications, Technologies, Architectures, and Protocols for Computer Communication (SIGCOMM '12)*. ACM, New York, NY, USA, 61–72. https://doi.org/10.1145/2342356.2342364 event-place: Helsinki, Finland.

[9] Michail E. Kiziroglou, David E. Boyle, Steven W. Wright, and Eric Yeatman. 2017. Acoustic power delivery to pipeline monitoring wireless sensors. *Ultrasonics* 77 (May 2017), 54–60. https://doi.org/10.1016/j.ultras.2017.01.017

[10] Nicolas Fourty, Adrien van den Bossche, and Thierry Val. 2012. An advanced study of energy consumption in an IEEE 802.15.4 based network: Everything but the truth on 802.15.4 node lifetime. *Computer Communications* 35, 14 (Aug. 2012), 1759–1767. https://doi.org/10.1016/j.comcom.2012.05.008

[11] Richard Primerano, Moshe Kam, and Kapil Dandekar. 2009. High bit rate ultrasonic communication through metal channels. In *2009 43rd Annual Conference on Information Sciences and Systems*. 902–906. https://doi.org/10.1109/CISS.2009.5054845

[12] Sijung Yang and Andrew C. Singer. 2016. Energy Efficient Ultrasonic Communication on Steel Pipes. In *2016 IEEE International Workshop on Signal Processing Systems (SiPS)*. 297–302. https://doi.org/10.1109/SiPS.2016.59

[13] STMicroelectronics. [n.d.]. TS882, TS884. https://www.st.com/resource/en/datasheet/ts882.pdf. Accessed: 2019-06-11.

[14] Vincent Liu, Aron Parks , Vamsi Talla, Shyamnath Gollakota, David Wetherall, and Joshua R. Smith. 2013. Ambient Backscatter: Wireless Communication out of Thin Air. In *Proceedings of the ACM SIGCOMM 2013 Conference on SIGCOMM (SIGCOMM '13)*. ACM, New York, NY, USA, 39–50. https://doi.org/10.1145/2486001.2486015 event-place: Hong Kong, China.